URSI GASS 2020, Rome, Italy, 29 August - 5 September 2020

An evaluation of Spire radio occultation data in assimilative ionospheric model GPSII and validation by ionosonde measurements

Kelsey K. Kramer(1), Sergey V. Fridman(1), and L. J. Nickisch(1)
(1) NorthWest Research Associates, Monterey, CA, 93940, http://www.nwra.com

Abstract

This paper presents the results of a comprehensive analysis of Spire Global, Inc.'s total electron content (TEC) observations using NorthWest Research Associate's (NWRA) assimilative ionospheric model GPSII. A week's worth of TEC data was collected from Spire's constellation of low-Earth orbiting micro-satellites carrying GNSS receivers and assimilated into GPSII. GPSII operation with the data was evaluated and the results were validated with observations from independent sources. Ground-based ionosondes were employed in diagnosing the accuracy of the derived models; NWRA studied the differences between the F2 peak parameters (f_0F_2 and H_mF_2) derived from ionograms and those computed with GPSII. The analysis showed that Spire's TEC data was both compatible for ingestion into GPSII and that the assimilation of the data improved the comparison to ground-based ionosondes. On average f_0F_2 was improved by 1.317 MHz and H_mF_2 was improved by 22.8 km with this data ingested into GPSII.

1 Introduction

Radio occultation (RO) TEC data has potentially great value for diagnostics of the state of the ionosphere [6]. GNSS-RO is a technique that uses GNSS signals received by low-Earth orbiting satellites to infer the distribution of electron density in the ionosphere. These lines-of-sight, between the GNSS satellites and satellites in low earth orbit (LEO), fall below the orbital paths of the LEO receivers. TEC derived from satellites in LEO is particularly relevant to ionospheric remote sensing due to both its unique geometrical look angles (compared to ground-based TEC data), and the capability to collect data over oceans, data-denied or inaccessible territories—such data may offer even greater value in defense-related applications. So far, the main issue that has been preventing this type of data to have a major impact on assimilative modeling of the ionosphere is related to sparsity of the existing data. The constellation of satellites that is being developed by Spire Global, Inc. promises to provide sufficiently dense coverage. In this paper we intend to explore the potential benefits of Spire's RO TEC data for the electron density model produced by GPSII.

2 Spire's Low Earth Orbit Multi-Use Receiver Cube-Satellite Constellation

Spire Global, Inc. is a space-to-cloud data and analytics company that designs, builds, and operates a constellation of 3U Cube-Satellites. Spire operates 88 satellites in LEO that collect a variety of RF signals, including Automatic Identification System (AIS), Automatic Dependent Surveillance Broadcast (ADS-B), and Global Navigation Satellite System (GNSS) data. The GNSS data volume can be broken down into subset data products, including RO and TEC for remote sensing of the neutral atmosphere and ionosphere, respectively. Each Cube-Satellite in Spire's constellation is capable of collecting a large volume of TEC measurements each day. Given that the GNSS receiver tracks approximately six dual-frequency GNSS satellites simultaneously, a single Spire Cube-Satellite is capable of recording well over 500,000 TEC measurements each day, assuming 100% duty cycle.

The dataset used in this research was delivered by the GNSS receivers flying onboard Spire's Low Earth Orbit Multi-Use Receiver (LEMUR) Satellite Bus. Spire provided data from 23 LEMUR-2 satellites, covering a full week. The data was collected at 1 Hz sampling rate and consists of relative TEC derived from GNSS phase delay measurements taken from July 25-31, 2019.

3 GPS Ionospheric Inversion (GPSII) Model

GPS Ionospheric Inversion, or GPSII, is NWRA's assimilative model of the ionosphere [4, 5]. This model is able to assimilate data from diverse sources, including various HF radio propagation measurements. In this study, we exploit GPSII capability to use TEC-related observations from one or more GNSS receiver to reconstruct a three-dimensional model of ionospheric electron density. These GNSS receivers can be ground-based, or satellite-mounted GPS receivers (such as on Spire's LEMUR satellites, or COSMIC satellites). Simultaneous measurements of multiple satellites by several GNSS receivers give TEC along different paths; GPSII uses a Tikhonov inversion algorithm to deconvolve the diverse measurements into a smooth, three-dimensional model.

4 Comparison of Model Results with Vertical Ionograms

A GPSII solution was obtained for four geographical regions, which will be referred to as "European," "North American," "North Pole," and "South American." These

regions were selected due to the large density of operating Digisonde and Dynasonde stations in the area during the week following July 25, 2019: 11 in the European region, 14 in the North American region, 22 in the North Pole region, and 8 in the South American region. The solutions cover a 7-day period with the step of 15 minutes starting at 00:00 UTC on July 25, 2019.

To evaluate the performance of Spire's TEC data assimilated into GPSII, the GPSII model results were compared to observations from independent sources. Vertical ionogram data was available for download from Digisonde [2] and Dynasonde [3] sounders and were employed in diagnosing the accuracy of the derived models. These ionograms were not assimilated in the ionospheric model; they were used purely for evaluation purposes. Assimilated data included only relative TEC data from GPS receivers mounted on LEMUR-2 Cube-Satellites.

NWRA investigated instances when the Spire LEMUR-2 Cube-Satellites sensed the ionosphere near a Digisonde or Dynasonde installations. This was accomplished by selecting cases in which the locations of the subionospheric points were in proximity (within a 1000 km radius, and 15 minutes in time) of an operating sounder. A subionospheric point is defined here as the "penetration point" where the receiver-satellite path used in the GPSII solution pierces the ionosphere at a 400 km altitude. This study identified 1,491 GPSII validation events between the four regions modeled that met these criteria. In each of these events, plasma frequency profiles were extracted from the GPSII solutions at the latitude and longitude of the given sounder station for the time of the event.

The key ionospheric parameters that can be reliably derived from ionograms and were used for assessment were 1) the F2 layer critical frequency, f_0F_2, and 2) the peak height of the F2 layer, H_mF_2. The magnitude of the deviation of the GPSII-predicted f_0F_2 or H_mF_2 at a sounder location, from the corresponding sounder-observed value was used as the measure of performance in this analysis. In order to evaluate whether or not the Spire data cause improvement of the GPSII solution, we compared the performance of the solution driven by Spire data to the solution obtained without assimilating any data. The latter model is the GPSII background model, which essentially reproduces the International Reference Ionosphere (IRI) [1].

5 Validation Results

An example of this comparison will be presented for the North American region and is illustrated in Figures 1-3. In Figure 1 is the GPSII-generated critical plasma frequency map for 04:00 UTC on July 30, 2019. This figure is representative of the data ingested into GPSII over a 15-minute period, from 03:45-04:00 UTC. In this example, there are several instances where Spire measurements were in proximity of an operating sounding station. Two of these cases will be presented here.

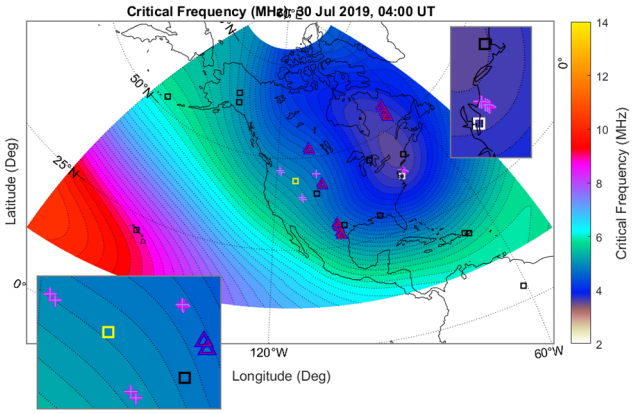

Figure 1. GPSII-generated geographical map of the critical plasma frequency for 04:00 UTC on July 30, 2019. Triangles signify the locations of the Spire satellite-based receivers. Crosses signify the subionospheric points; they are representative of the measurements of multiple GPS satellites that were taken by the Spire receivers. Squares signify the locations of local Digisonde or Dynasonde stations; they are included for visualization purposes only, as these stations and their data were not employed in the GPSII solution. The yellow square is the IF843 Digisonde station. The white square is the WP937 Digisonde station.

The first case takes place at the Idaho National Lab Digisonde station (IF843). The distance between IF843 and the nearest subionospheric point is 661.5 km. The GPSII plasma frequency profiles at this Digisonde location for this data and time can be seen in Figure 2a and the ionogram recorded at this Digisonde station can be seen in Figure 3a. The Digisonde-observed value for f_0F_2 at this station was 4.875 MHz. In the case of the GPSII solution obtained without assimilating any data, the maximum plasma frequency of the profile (blue trace in Figure 2a) was 5.399 MHz. With Spire data assimilated, the maximum plasma frequency of the GPSII-generated profile (orange trace in Figure 2a) was 4.987 MHz. Which is an improvement on the background solution, off by only 0.112 MHz. As for H_mF_2, the ionogram-derived value is 259.4 km. In the case of the GPSII solution obtained without assimilating any data, the peak height of the F2-layer was 295 km. With Spire data assimilated, GPSII more accurately calculates the value to be 265 km; bringing the magnitude of the deviation down from 35.6 to 5.6 km.

The second case takes place at the Wallops Island, VA Digisonde station (WP937). The distance between WP937 and the nearest subionospheric point is 182.5 km. The GPSII plasma frequency profiles at the Wallops Island Digisonde location for 04:00 UTC on July 30, 2019 can be seen in Figure 2b and the ionogram recorded at this Digisonde station can be seen in Figure 3b. The Digisonde-observed value for f_0F_2 at this station was 3.400 MHz and for $H_mF_2$was 281.7 km. In the case of the GPSII solution obtained without assimilating any data, the maximum plasma frequency of the profile (blue trace in Figure 2b)

was 5.047 MHz and the peak height of the F2-layer was 320 km. With Spire data assimilated, the maximum plasma frequency of the GPSII-generated profile (orange trace in Figure 2b) was 3.694 MHz and the peak height of the F2-layer was 280 km. Another improvement, the Spire-driven GPSII solution is off by just 0.294 MHz and 1.7 km.

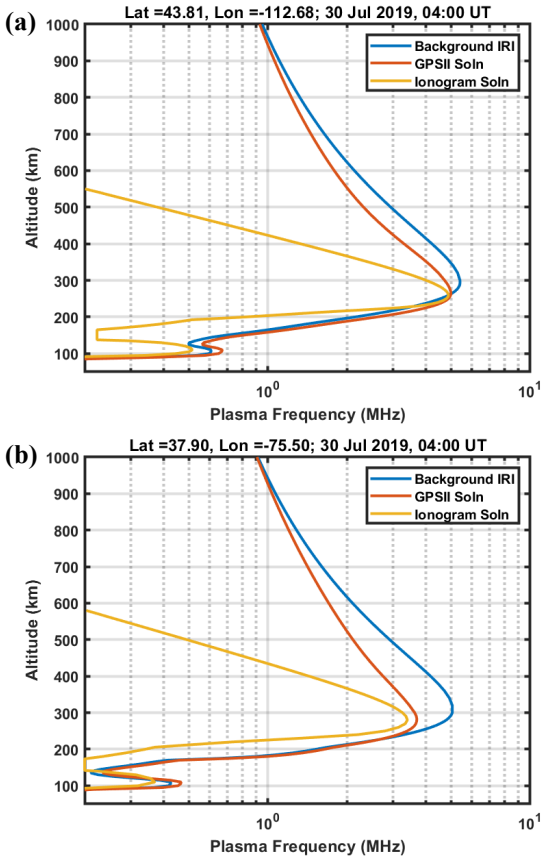

Figure 2. Plasma frequency profiles at the **(a)** Idaho National Lab Digisonde station (IF843) and **(b)** Wallops Island Digisonde station (WP937) at 04:00 UTC on July 30, 2019. In blue is the background IRI profile (GPSII-generated plasma frequency profile with no data ingested), in orange is the GPSII solution profile (GPSII-generated plasma frequency profile with only Spire TEC data ingested), and in yellow is the plasma frequency profile put out in DIDBase.

6 Summary

A summary of the differences between the critical frequencies and the peak heights of the F2 layer in GPSII solutions and the corresponding ionogram observations can be found in Table 1. For the 1,491 validation events used in this study, the magnitude of the deviation of the GPSII-predicted f_0F_2 at a Digisonde (or Dynasonde) location from the corresponding sounder-observed value was found on average to be 0.608 MHz (with a median of 0.461 MHz). Whereas the deviation between the critical frequencies in the background IRI-predicted f_0F_2 profiles and the sounders was found on average to be 1.924 MHz (median value of 1.807 MHz). Of the 1,491 validation events, in only 84.31% was H_mF_2 reliably derived from the sounders. For those, the magnitude of the deviation of the GPSII-predicted H_mF_2 at a sounder location from the corresponding sounder-observed value was found to be on average 22.9 km (with a median value of 18.0 km). Whereas the deviation between the background IRI-predicted peak height of the F2-layer and the sounder-derived values was found on average to be 45.7 km (median value of 38.8 km). The distributions of deviations for f_0F_2 and H_mF_2 can be seen in Figure 4. Thus, with a statistically significant data set, it has been shown that including relative TEC from radio occultation data from Spire generally improved the accuracy of GPSII's prediction of f_0F_2 and H_mF_2 . It means that TEC observations from LEO-satellite mounted GPS receivers substantially improve GPSII prediction of the bottom-side F-region of the ionosphere.

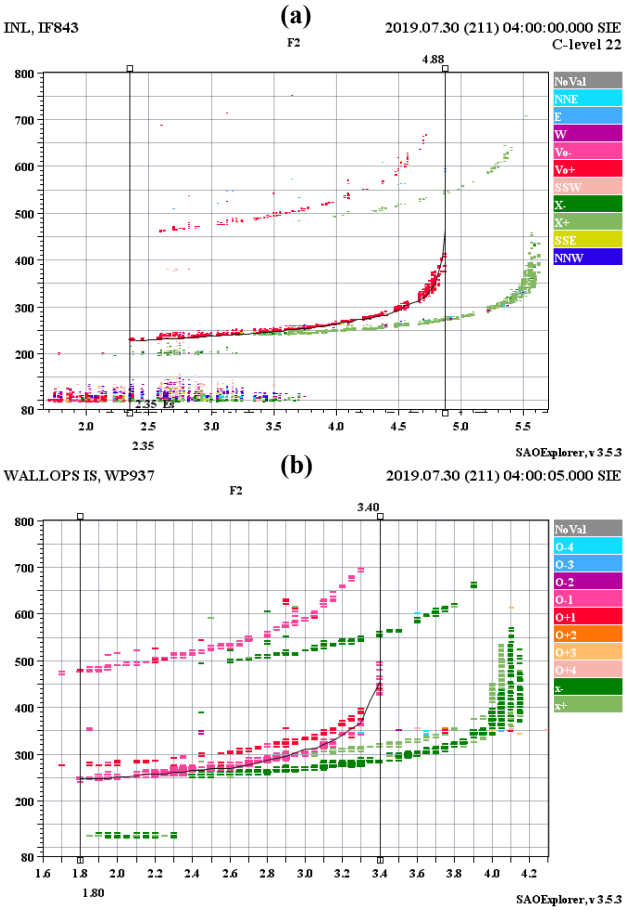

Figure 3. Ionograms from the **(a)** Idaho National Lab and **(b)** Wallops Island Digisonde stations at 04:00 UTC on July 30, 2019.

Table 1. Summary of differences between the critical frequencies, f_0F_2 (MHz), and the peak heights of the F2 layer, H_mF_2 (km), in GPSII solutions and the corresponding ionogram observations. Values based on background IRI in blue and values based on Spire-driven GPSII solutions in orange:

Differences between the critical frequencies, f_0F_2, and corresponding ionogram observations (MHz):

	European		North American		North Pole		South American		OVERALL	
	From IRI	From Soln	From IRI	From Soln	From IRI	From Soln	From IRI	From Soln	From IRI	From Soln
Max	3.895	2.467	3.417	1.890	3.896	2.469	5.407	3.229	5.407	3.229
Min	0.748	0.001	0.062	0.001	0.055	0.001	0.656	0.025	0.055	0.001
Mean	1.967	0.686	1.575	0.479	1.747	0.512	3.003	1.002	1.924	0.608
Median	1.925	0.585	1.509	0.368	1.712	0.398	3.005	0.901	1.807	0.461
# of Cases	342		285		675		189		1491	

Differences between the peak height of the F2 layer, H_mF_2, and corresponding ionogram observations (km):

	European		North American		North Pole		South American		OVERALL	
	From IRI	From Soln	From IRI	From Soln	From IRI	From IRI	From Soln	From IRI	From Soln	From IRI
Max	129.4	98.1	142.7	90.7	142.7	118.1	107.8	76.4	142.7	118.1
Min	1.0	0.1	1.3	0.1	0.8	0.1	1.3	0.1	0.8	0.1
Mean	42.8	22.7	47.8	24.3	47.1	22.2	42.9	23.4	45.7	22.9
Median	38.7	18.3	36.9	16.4	39.7	18.3	39.0	17.3	38.8	18.0
# of Cases	284		239		559		175		1257	

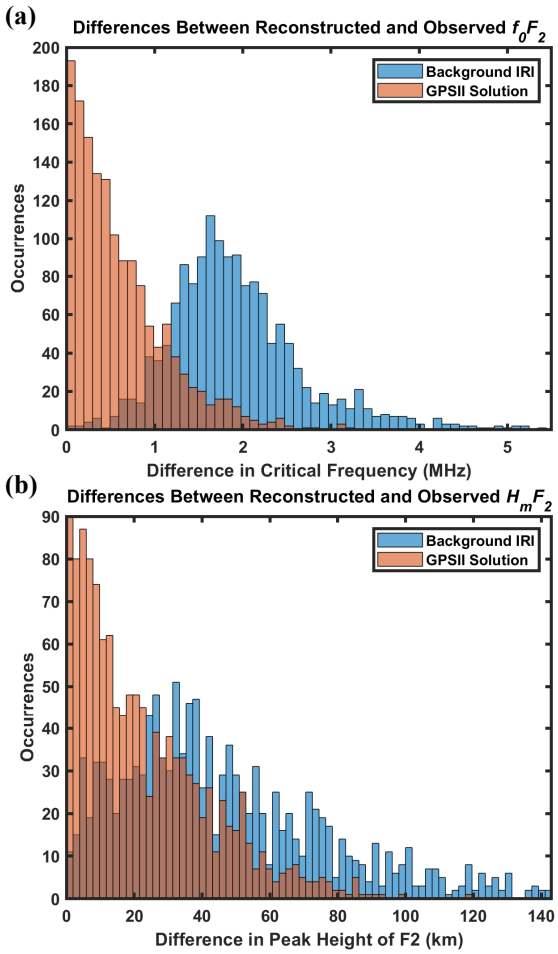

Figure 4. Histograms of the magnitude of deviation of **(a)** the f_0F_2 extracted with GPSII at a sounder location, from the corresponding sounder-observed value and **(b)** the H_mF_2 extracted with GPSII at a sounder location, from the corresponding sounder-observed value. Values based on background IRI in blue and values based on Spire-driven GPSII solutions in orange.

7 Acknowledgements

The authors would like to express their gratitude to Spire Global, Inc. (https://spire.com/en/spire/about-spire) for providing LEMUR-2 Cube-Satellite constellation data. This work was supported by DARPA under Contract No. 140D6319C0032. Any opinions, findings and conclusions or recommendations expressed in this material are those of the authors and do not necessarily reflect the views of DARPA.

8 References

[1] D. Bilitza, D. Altadill, Y. Zhang, C. Mertens, V. Truhlik, P. Richards, L. McKinnell, and B. Reinisch, "The International Reference Ionosphere 2012 – a Model of International Collaboration," *Journal of Space Weather and Space Climate*, **4**, A07, February 2016, https://doi.org/10.1051/swsc/2014004.

[2] "DIDBase - Digital Ionogram Database." 2019, Accessed 2019, https://ulcar.uml.edu/DIDBase/.

[3] "Dynasonde Database." 2019, Accessed 2019, http://surf.colorado.edu/login.dcc.

[4] S. V. Fridman, L. J. Nickisch, and M. Hausman, "Personal-Computer-Based System for Real-Time Reconstruction of the Three-Dimensional Ionosphere Using Data from Diverse Sources," *Radio Science*, **44**, 3, June 2009, https://doi.org/10.1029/2008RS004040.

[5] S. V. Fridman, L. J. Nickisch, M. Hausman, and G. Zunich, "Assimilative Model for Ionospheric Dynamics Employing Delay, Doppler, and Direction of Arrival Measurements from Multiple HF Channels: Assimilation of HF Measurements," *Radio Science*, **51**, 3, February 2016, pp. 176–83, https://doi.org/10.1002/2015RS005890.

[6] W. S. Schreiner, S. V. Sokolovskiy, C. Rocken, and D. C. Hunt, "Analysis and Validation of GPS/MET Radio Occultation Data in the Ionosphere," *Radio Science*, **34**, 4, July-August 1999, pp. 949–66. https://doi.org/10.1029/1999RS900034.